Internal Friction Controls the Speed of Protein Folding from a Compact Configuration[†]

Suzette A. Pabit,[‡] Heinrich Roder,[§] and Stephen J. Hagen*,[‡]

*Department of Physics, University of Florida, P.O. Box 118440, Gainesville, Florida 32611-8440, and
Fox Chase Cancer Center, Basic Science Division, 333 Cottman Avenue, Philadelphia, Pennsylvania 19111*

ABSTRACT: Several studies have found millisecond protein folding reactions to be controlled by the viscosity of the solvent: Reducing the viscosity allows folding to accelerate. In the limit of very low solvent viscosity, however, one expects a different behavior. Internal interactions, occurring within the solvent-excluded interior of a compact molecule, should impose a solvent-independent upper limit to folding speed once the bulk diffusional motions become sufficiently rapid. Why has this not been observed? We have studied the effect of solvent viscosity on the folding of cytochrome *c* from a highly compact, late-stage intermediate configuration. Although the folding rate accelerates as the viscosity declines, it tends toward a finite limiting value $\sim 10^5$ s^{-1} as the viscosity tends toward zero. This limiting rate is independent of the cosolutes used to adjust solvent friction. Therefore, interactions within the interior of a compact denatured polypeptide can limit the folding rate, but the limiting time scale is very fast. It is only observable when the solvent-controlled stages of folding are exceedingly rapid or else absent. Interestingly, we find a very strong temperature dependence in these "internal friction"-controlled dynamics, indicating a large energy scale for the interactions that govern reconfiguration within compact, near-native states of a protein.

The folding of a protein requires both large-scale diffusion of the polypeptide chain and smaller, more local reconfigurations of the backbone and side chains. A number of studies in recent years have attempted to determine which types of motions actually constitute the rate-determining step of folding (*1−7*). These studies have addressed this question by examining the effect of solvent viscosity on the rate of folding: They have typically found that the folding time increases in direct proportion to the solvent viscosity, just as the diffusion of a free particle slows in a viscous solvent. This supports the idea that the bulk diffusional steps control the speed of folding. One can argue, however, that the folding of a polypeptide proceeds on such a small length scale and with such weak forces that its dynamics cannot be controlled by anything except diffusion. Constant molecular collisions give rise to drag or friction that impedes all motion of the polypeptide and its side chains. These same collision forces manipulate the main chain and side chains into the proper native fold. From this perspective, the key result from the viscosity studies is not that folding is rate-limited by diffusion; rather, these studies show that the molecular forces that control folding speed arise almost entirely from the solvent. In fact, a simple macroscopic property of the solvent—its viscosity—sets the time scale for the microscopic dynamics of folding.

This result is suprising, because many proteins are known to fold via highly compact transition states. Within such compact states, from which solvent is largely excluded, one might expect interactions within the polypeptide and between side chain atoms to influence the dynamics much more strongly than does the surrounding solvent. Why does the folding instead appear closely coupled to the solvent? We have investigated this question by studying a very rapid (~ 10 μs) folding process that occurs in a highly compact configuration of horse cytochrome *c*. We find that the dynamics of this fast folding are largely decoupled from the solvent, so that their speed is controlled by interactions internal to the polypeptide chain. We conclude that the internal reorganizations that are governed by intrachain interactions proceed on a very rapid time scale. They constitute the rate-limiting stage of folding only when other stages are either absent or else exceptionally fast.

Frictional Control of Folding Reactions. Kramers theory for unimolecular reaction rates provides a framework for understanding diffusion-controlled, barrier-crossing processes such as protein folding (*5, 8−11*). Kramers theory asserts that the rate k_f for a heavily damped process depends on both the activation free energy ΔG_a and a reaction friction parameter γ, through $k_f \propto \gamma^{-1} \exp(-\Delta G_a/k_B T)$. This predicts that the folding rate for a polypeptide should scale inversely with the friction γ. This prediction is supported by computer simulations (*10, 12*). However, the theory does not specify the physical origin of the friction. One key physical question

* To whom correspondence should be addressed. Tel. 352-392-4716. Fax: 352-392-7709. E-mail: sjhagen@ufl.edu.
[‡] University of Florida.
[§] Fox Chase Cancer Center.

is, what is the source of the friction γ that controls the speed of folding?

In the simplest interpretation, the friction arises because bulk motion of the polypeptide chain is impeded by the solvent, which has a dynamic viscosity η_s. Then, γ is controlled by η_s, and from Kramers, we expect $k_f \propto \eta_s^{-1}$. A number of authors have tested this model (*1–6, 13–16*) by adding viscogenic cosolutes to refolding buffers and measuring the effect on the folding rate of various proteins. These studies present experimental difficulties, because the cosolutes typically shift the stability of the protein's native state (*1, 2*), they may also give rise to discrepancies between the microscopic and the macroscopic viscosity of the solvent (*17, 18*). However, in studies where these effects are carefully controlled while η_s is varied, the expected inverse viscosity behavior has been observed in folding rates. In general, the folding rate shows no deviation from perfect solvent-controlled behavior: k_f^{-1} is linear in η_s and extrapolates toward zero as $\eta_s \to 0$ (*3–6*). Thus, the folding rate k_f behaves as if it would grow without limit as the solvent viscosity declines.

One must question how this can be correct. Kinetics studies probe only the rate-limiting diffusional passage over the primary barrier; this diffusion may continue to accelerate as η_s decreases, but other fast dynamics that couple less strongly to the solvent environment should eventually become rate limiting and should exert control over k_f at sufficiently small η_s. For example, late-stage reconfigurations within a compact globule, with a minimal solvent accessible surface, should show less dependence on solvent viscosity. The time scale of these internal reconfigurations, even if very rapid, would set a finite limit to the folding rate and thus cause k_f to deviate from simple η_s^{-1} behavior at low solvent viscosities, $\eta_s \to 0$.[1] Such limiting behavior has been observed in the conformational relaxations of (folded) myoglobin at low solvent viscosity (*19*) and is anticipated in theoretical descriptions of folding (*11*).

More precisely, theory and experiment in polymer dynamics suggest that both solvent friction and "internal friction" influence the dynamics of chain molecules. Internal friction is a generic term for a variety of damping interactions arising primarily within the chain, rather than directly from the solvent viscosity (*11, 12, 20–23*). Although different theoretical models differ in details, it has been suggested that an internal friction contribution to γ should cause folding rates to depart from $k_f^{-1} \propto \eta_s$ and approach a finite limit at sufficiently small η_s (*3, 11, 15*). One cannot experimentally access the regime $\eta_s \ll \eta_{water}$ in order to test this directly. One can, however, examine whether k_f^{-1} is strictly proportional to η_s when $\eta_s \approx \eta_{water}$ or whether it deviates[2] such as by extrapolating toward a nonzero limiting folding time k_f^{-1} at low η_s. Most such extrapolations show no clear

evidence for an internal friction limit to folding speed. However, a recent study showed that the folding time of the ultrafast-folding Tryptophan Cage [$k_f \approx (3\ \mu s)^{-1}$ in water] tends toward a finite value ($\sim 0.7\ \mu s$) in the limit of low η_s (*25–27*). This result showed that internal friction can detectably influence the fastest folding systems.

Here we show that for very rapid folding from a compact state, the internal interactions of the protein can exert strong control over folding speed. We have studied the rapid folding of a compact non-native form of Fe^{2+}-cytochrome *c*. Because folding from this compact state begins after the collapse from a fully unfolded state, the dynamical effects of internal friction are directly measurable. The compact state is prepared from chemically denatured cytochrome *c* by lowering the denaturant concentration in the presence of carbon monoxide, which binds tightly to the heme iron and prevents formation of the native Met80-heme (sulfur–iron) link (*28–30*). Laser flash photolysis of the CO-iron bond in this metastable intermediate then triggers folding to the native state. We used transient absorption spectroscopy to observe this rapid ($k_f \sim 10^5\ s^{-1}$) process. Its solvent viscosity dependence reveals fast dynamics that respond only weakly to the solvent properties, indicating that they are controlled primarily by internal interactions. These dynamics in fact account for most of the temperature dependence in k_f, suggesting that substantial intrachain interaction energies control the configurational diffusion within the compact molecule.

MATERIALS AND METHODS

M-CO State of Horse Cytochrome c. Unfolding Fe^{2+}-cytochrome *c* at a high denaturant concentration breaks the covalent link between the heme iron and its native ligand (the sulfur of Met80) and allows exogenous ligands such as carbon monoxide to bind to the heme (*29, 31*). While Fe^{2+}-cytochrome *c* undergoes a highly cooperative unfolding transition at very high denaturant concentrations indicative of an unusually stable protein (~ 71 kJ/mol), the addition of CO results in a dramatic decrease in stability, by ~ 38 kJ/mol (*30*), and major deviations from a two-state unfolding transition (*28, 29*).

Detailed equilibrium studies of the solvent-induced unfolding transition of horse Fe^{2+}-cytochrome *c* in the presence of CO, using heme absorbance, circular dichroism (CD), and fluorescence methods, revealed a highly populated ($\sim 75\%$) intermediate state, M-CO, at moderate denaturant concentrations, characterized by a red-shifted heme absorption (Soret) band, near-native far-UV CD spectrum, and weak Trp-59 fluorescence due to Förster transfer to the heme. Recent NMR data on a uniformly ^{15}N-labeled sample of Fe^{2+}-cytochrome *c* in its metastable M-CO state (in the absence of denaturant) showed a well-dispersed $^1H–^{15}N$ correlation spectrum with extensive chemical shift perturbations relative to native Fe^{2+}-cytochrome *c* (*28*).

Thus, M-CO represents a compact, highly structured state with nativelike helix content but non-native tertiary structure and heme coordination. At room temperature, the CO thermally dissociates and escapes from the protein with a time constant $\tau \sim 1$ h at 20 °C. An external light pulse can also break the heme-CO bond, allowing the CO to escape. This converts M-CO into a structurally equivalent pentaco-

---

[1] Extrapolation to $\eta \ll \eta_{water}$ does not imply that we are studying the rate of protein folding in zero solvent viscosity. Experimentally, one can only observe folding dynamics in the high friction limit of Kramers. The extrapolation is simply a practical method for identifying the contribution of the protein's internal friction to the total reaction friction.

[2] Deviations from Kramers' $k \propto 1/\gamma$ may also occur if the barrier crossing occurs quickly enough to approach the molecular reorganization time of the solvent (*24*). This scenario appears unlikely in a protein folding reaction.

ordinate state M, which then folds rapidly to the native (N) state. In contrast to previous studies that found no evidence for structural intermediates in the folding process of reduced cytochrome c (*30, 32*), our recent rapid mixing results show clear deviations from two-state folding/unfolding kinetics both at low and at high denaturant concentrations consistent with a four-state mechanism featuring both early and late folding intermediates (Maki, K., Latypov, R. F., Cheng, H., Luck, S. D., S. A. P., S. J. H., and H. R., to be submitted). The results confirm that a nativelike state, M, occurs even in the absence of CO.

Preparation of the M-CO Samples. Lyophilized horse cytochrome c (Sigma Chemical Co.) was dissolved into 6 M Gdn-HCl and 0.1 M Tris, pH 7.0, and deoxygenated by a flow of O_2-free CO at 1 atm, with ~1 mM sodium dithionite added to reduce the heme iron to Fe^{2+}. This forms the CO complex of unfolded Fe^{2+}-cytochrome c. Diluting this mixture into a CO-saturated buffer collapses the protein into the M-CO state, in which the CO ligand remains in the iron site, displacing the Met80 sulfur. Final denaturant concentrations were 0.5−2 M Gdn-HCl.

Viscosity Measurements. The dilution buffer also contained cosolutes—glycerol, ethylene glycol, or glucose—at concentrations sufficient to raise the dynamic viscosity η_s as much as 5−6-fold, and a glucose/oxidase/catalase mixture to scavenge any remaining O_2 (*34*). Solutions for viscosity studies therefore contained 50 μM cytochrome c, 0.5 M Gdn-HCl, a viscogenic cosolute, the enzyme system ($\leq$0.32 μM glucose oxidase, $\leq$3.5 μM catalase, and 0.3% glucose), and sodium dithionite. We directly measured (*33*) the kinematic viscosity η_s/ρ of each mixture at each temperature, using a calibrated Cannon-Fenske viscometer fully immersed in a water bath, for an accuracy of $\pm$0.1%. Lavalette and co-workers have shown that low molecular weight cosolutes of the type used here raise both the microscopic (i.e., as seen by the protein) and the macroscopic (i.e., bulk) solvent viscosity. Large polymeric viscogens, such as PEG, may only raise the macroviscosity (*17, 18*).

Optically Triggered Protein Folding. We use transient absorption spectroscopy to study the folding M → N. Folding is triggered by dissociating the CO from M-CO with a laser pulse and is observed through heme absorbance changes in the visible Soret region as the Met80 sulfur rebinds to the heme. The transient spectrometer, described elsewhere (*35, 36*), uses a 5−7 ns laser pulse at 532 nm to photodissociate the CO from the heme iron and collects a series of visible absorption difference spectra at time intervals from ~10 ns to >1 s following photolysis. We use singular value decomposition (SVD) to analyze the difference spectral data: At these low denaturant concentrations ($\leq$2.4 M Gdn-HCl), each data set contains two SVD components, each describing the same two relaxations. Relaxation rates are determined through a biexponential fit to the first two SV amplitudes. The first relaxation (rate $k_f \sim 10^5$ s^{-1}) represents spectral changes corresponding to the folding transition M → N. The second (with rate ~ 3 s^{-1}) corresponds to the replacement of folded by denatured protein, as a syringe pump supplies fresh sample to the optical cell. Uncertainties in the rates were estimated by the Monte Carlo bootstrap method. The estimated error bars tend to increase at high solvent viscosity, where the slower diffusion of the CO ligand tends to favor greater geminate recombination and therefore gives a smaller net photolysis signal.
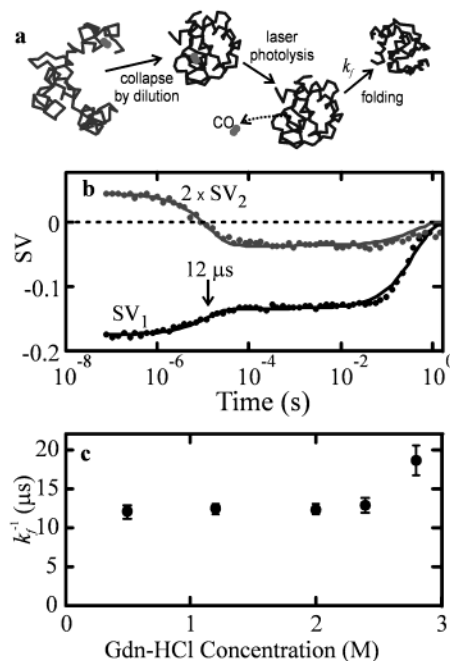

FIGURE 1: Folding from a collapsed state. (a) Schematic of the folding process. Unfolded CO-cytochrome c at high Gdn-HCl (far left) collapses to the metastable M-CO state upon dilution into buffer. Laser flash photolysis dissociates the CO molecule from the heme to give the M state, which folds to the native state N (far right) at rate k_f. (b) The amplitudes $SV_1(t)$ and $SV_2(t)$ of spectral changes obtained by SVD of transient absorption spectra following photolysis and biexponential fit giving relaxation rates. The sample contained 1.2 M Gdn-HCl, $T = 20$ °C. The first relaxation ($k_f^{-1} \approx$ 12 μs) represents spectral changes corresponding to the folding transition M → N. The second (with rate ~ 3 s^{-1}) corresponds to the replacement of folded by denatured protein, as a syringe pump supplies fresh sample to the optical cell. (c) Denaturant concentrations up to ~2.5 M Gdn-HCl do not affect folding time k_f^{-1} at 20 °C.

RESULTS

Because equilibrium strongly favors the folded N state over the compact denatured states M and M-CO at low denaturant concentrations, the rate of relaxation following photolysis of CO corresponds to the rate of folding (k_f) with minimal contributions from unfolding (Figure 1). Folding requires both configurational diffusion of the compact, denatured protein and a chemical reaction between the ferrous heme and its native ligand, the sulfur atom of Met80. This chemical reaction is known to occur at a geminate rate $k_g \approx 4 \times 10^{10}$ s^{-1} at 22 °C (and $k_g \approx 10^{11}$ s^{-1} at 40 °C) (*37*), which far exceeds the microsecond folding rates observed here. Hence, the folding rate k_f is not limited by chemical bond formation. Instead, k_f characterizes the rate of reconfigurations of the polypeptide chain that bring Met80 into contact with the pentacoordinate heme.

Figure 1 shows typical kinetic traces obtained from the transient absorption spectroscopy, where the rapid (12 μs) relaxation corresponds to the folding transition M → N. In a Kramers theory description of a two-state protein folding reaction, the rate of folding depends on both the reaction friction γ and the height of the activation free energy barrier ΔG_a. Studies of viscosity effects on folding must therefore account for the influence of viscogenic cosolutes on the stability of the native state, because similar shifts in ΔG_a may generate an extra perturbation to k_f (*1−6, 14−16, 38*).
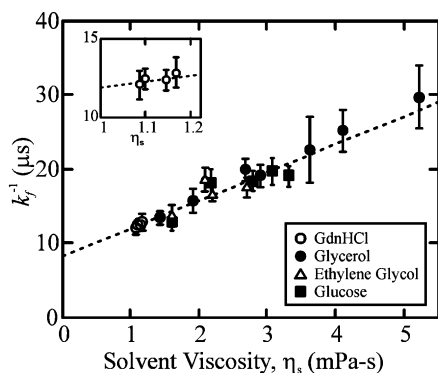
FIGURE 2: Viscosity dependence of M → N folding time at 20 °C. The figure shows that data for different viscogens—including glycerol (●), ethylene glycol (△), and glucose (■) (all in 0.5 M Gdn-HCl), as well as for 0.5−2.4 M Gdn-HCl (○) with no extra viscogen—all follow the same linear dependence. The inset magnifies the low viscosity region, showing data at a variable Gdn-HCl concentration. Pure water has viscosity = 1 mPa s = 1 cP at 20 °C.

Previous authors have used different methods to compensate for these ΔG_a shifts, such as adding denaturant simultaneously with the viscogen (*3*) or choosing experimental conditions where the cosolute does not affect ΔG_a (*6*). In the present case, Figure 1 shows that the rate of transition k_f from the intermediate (M) to the folded (N) state shows no sensitivity to the overall free energy of folding, ΔG. Figure 1c shows that k_f remains unaffected by Gdn-HCl concentration over the range 0−2.4 M, even as $\Delta G = G_M − G_N$ decreases from 17 kJ/mol to 0 (*28*). The very weak effect on k_f {with $\partial \ln k_f/\partial$ [Gdn-HCl] ≈ (0.02 ± 0.05) M^{-1}} indicates that any destabilization of the native state (such as from Gdn-HCl or other cosolutes) does not affect the activation free energy of folding, ΔG_a; the solvent-exposed surface area does not change as the protein passes from the M state to the folding transition state.[3] Therefore, the data do not require compensation for viscogen effects on ΔG.

Three different viscogens (glycerol, glucose, and ethylene glycol) had a similar slowing effect on the folding kinetics, causing the same linear increase in k_f^{-1} with solvent viscosity (Figure 2). This result is consistent with the expectation of a linear dependence, $k_f^{-1} \sim \eta_s$; however, a linear extrapolation to low viscosity, $\eta_s \to 0$, clearly indicates a finite limiting value $k_f^{-1}(0) \approx 8.10 ± 0.63$ μs at 20.0 ± 0.2 °C. In fact, Figure 2 shows that this limiting folding rate k_f (0) only moderately exceeds (by 50%) the rate in water ($\eta_{water} = 1$ mPa s). Unlike the folding observed in many other systems, the dynamics that control k_f here couple weakly to the solvent friction.

DISCUSSION

Kramers theory for folding predicts that the folding rate k_f will vary inversely with the microscopic friction γ. If the friction is due to the viscosity η_s of the solvent, then a plot of k_f^{-1} vs η_s will follow a straight line that extrapolates through the origin ($k_f^{-1} = 0$) as $\eta_s \to 0$. This is the behavior observed in most previous studies, conducted on relatively slowly (ms → s) folding proteins. However, a recent study

---

[3] Figure 2 (inset) shows that the increase in the solvent viscosity due to rising [Gdn-HCl] may even account for the small variation of k_f. $\partial \ln (1/\eta)/\partial$[Gdn-HCl] ≈ −0.05 M^{-1}.

of a small, ultrafast folding protein (TrpCage Tc5b, $k_f \approx 3 \times 10^5$ s^{-1}) showed that the folding of that protein departs slightly from $k_f^{-1} \propto \eta_s$. That is, while the folding time k_f^{-1} varies linearly with solvent viscosity, it exhibits a positive intercept, so that the folding rate tends toward a limiting value $\sim 1.5 \times 10^6$ s^{-1} at low solvent friction (*25*). Some deviation has also been observed in the very rapid (10^{-7} s) dynamics of α-helix formation (*15*). This implies that other interactions not coupled to solvent do set a finite—although very rapid—limit on folding rates. The present data support this view: Figure 2 shows that a highly compact metastable state of cytochrome *c* folds rapidly ($\sim$10 μs) but that this rate varies only weakly with solvent viscosity. Because the folding dynamics appear largely decoupled from the solvent viscosity, interactions internal to the compact molecule must control the diffusional reconfigurations that occur. Such interactions are known in the polymer dynamics literature as internal friction (*11, 20, 21*).

The concept of internal friction has a long history. Early dynamical experiments on polymer chains showed that rheological and viscoelastic properties of macromolecules can be interpreted in terms of two contributions to the frictional force: solvent friction and an additional internal friction (*20, 21, 39, 40*). There exist a number of possible mechanisms by which a polymer chain could experience drag forces that do not simply result from the bulk viscosity of the solvent (*20, 21*). These can include potential energy barriers to backbone rotations, long-range (i.e., sequence distant) interresidue interactions, and the accessibility of free volume in a noncontinuum solvent. For example, any reconfiguration of a polymer chain requires the backbone bonds to turn through their rotational potential, and this constitutes a dissipative process that adds to the simple solvent drag.

Different models for the internal friction phenomenon predict different consequences for the chain dynamics. De Gennes suggested (*20*) that the relaxation time for a polymer chain consists of two contributions, $\tau = \tau_s (\eta_s) + \tau_{int}$, where $\tau_s (\eta_s)$ is the relaxation time associated with solvent-damped motion of the polymer, while τ_{int}—which is independent of η_s—reflects the dynamics controlled by internal friction. In this view, measurements of τ extrapolated to low η_s will reveal the time scale τ_{int} for the internal friction-controlled dynamics. Although we are not aware of a detailed modern theory for internal friction effects in protein folding, the general suggestion from ref (*20*) that relaxation or folding time may extrapolate to a finite limit at low η_s is preserved in some recent theoretical treatments of protein folding (*11*), and it appears consistent with previous data on protein conformational relaxations (*19*); see below. It is also consistent with our data.

Ansari and co-workers (*19*) studied nanosecond conformational dynamics in (folded) myoglobin and found evidence for a finite relaxation rate at low η_s. They proposed an empirical, additive friction model to incorporate an internal friction contribution into a Kramers-like model for the relaxation dynamics:

$$k = A(\sigma + \eta_s)^{-1} \exp(-\Delta G/k_B T), \qquad (1)$$

Here, σ describes a "protein friction" associated with the conformational relaxation. The total reaction friction is then

$\gamma \propto \sigma + \eta_s$ so that k extrapolates to a constant (determined by σ) at low η_s. Applying eq 1 to their data produced a substantial value $\sigma = 4.1 \pm 1.3$ mPa s or about 4× larger than the viscosity of water. However, several attempts to fit eq 1 to protein folding data have found no clear evidence for $\sigma > 0$, even for proteins that fold through compact transition states. For the folding of protein *L*, the near-linearity of k_f with respect to $1/\eta_s$ for 1 mPa s $\leq \eta_s \leq 3.5$ mPa s implies $\sigma \approx -0.1 \pm 0.2$ mPa s in eq 1, a result that suggests no protein friction in folding (*3*). The data of Jacob et al. also imply a very small σ for CspB (*6*). However, for the M → N folding of cytochrome *c*, the data of Figure 2 clearly extrapolate toward an *x*-intercept ($-\sigma$) that is significantly different from zero, i.e., $\sigma \approx 2.1 \pm 0.3$ mPa s.

We suggest that the protein friction parameter σ does not provide the best measure of friction effects in folding. First, it is unclear how to interpret σ, which has units of macroscopic viscosity (mPa s), as a measure of a microscopic phenomenon. Second, kinetic studies probe only the rate-limiting step, so that even a large σ associated with a rapid process would not be detected if a slower process with $\sigma = 0$ limits the overall folding rate. We argue that the folding time in the limit of small solvent viscosity (i.e., the *y*-intercept of Figure 2) gives a clearer indicator of the internal friction contribution to the dynamics, as it has a fairly simple interpretation as the speed of the rate-limiting step when the bulk diffusional motions of the chain (such as loop or sheet formation) become extremely rapid. For example, although the data of refs (*3*, *6*) imply that $\sigma \approx 0$ in the folding of protein *L* and CspB, they certainly do not suggest that $k_f^{-1} \rightarrow 0$ as $\eta_s \rightarrow 0$; given the time resolution of those data, one can only conclude that the rate-limiting step of folding at low η_s requires at least a few milliseconds. The data do not rule out a limiting folding rate $\sim 10^5$ s^{-1}, as appears in Figure 2.

To emphasize this limiting time scale in the folding data of Figure 2, we consider the folding time as the sum of two separate time scales.[4]

$$k_f^{-1} \approx \tau_s + \tau_{int} \qquad (2)$$

Here, $\tau_s \propto \eta_s$ describes the time scale for solvent-controlled reorganizations of the polypeptide. It is responsible for the Kramers-like response to bulk solvent viscosity. The second time scale τ_{int} characterizes dynamics controlled by internal friction and insensitive to solvent viscosity. It determines the finite limiting value of k_f. For example, folding from the M state may require a reorganization of solvent-exposed regions of the molecule, followed by a substantial reconfiguration within the compact interior—with little displacement of the surrounding solvent. Depending on the magnitude of η_s, either set of motions may control the overall time for folding. As a mathematical description of the k_f data, eq 2 is equivalent to the protein friction model of Ansari et al.—both models describe k_f^{-1} as linear in η_s but with a finite intercept. However, they differ significantly in interpretation. Eq 2 characterizes the effect of internal friction not as an

---

[4] One cannot fit the data to an obvious alternative, the additive rate model $k_f = 1/\tau_s + 1/\tau_{int}$ where $\tau_s \sim \eta$. This is because the folding rate remains finite as $\eta \rightarrow 0$, whereas the rate $1/\tau_s$ would diverge in this limit.
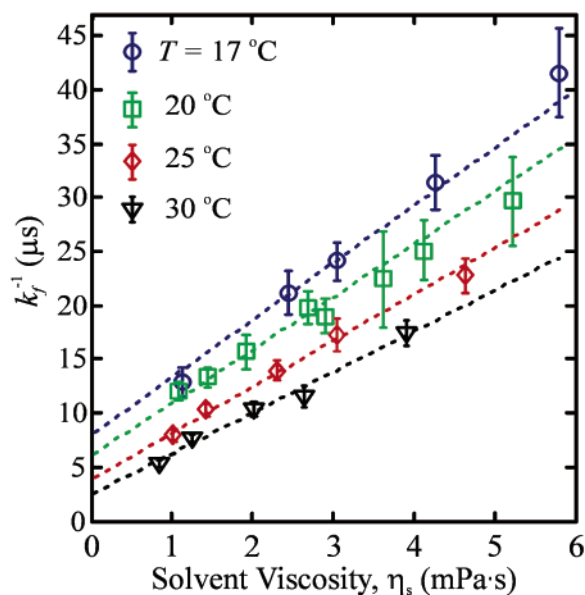

FIGURE 3: Temperature and viscosity effects on the folding time k_f^{-1}. Solvent viscosities vary strongly with temperature, but the indicated viscosities refer to the dynamic viscosity of the sample solvent, directly measured at the indicated temperature. Temperature changes have a more substantial effect on the intercept than on the slope. (For clarity, the figure shows only data collected in glycerol/Gdn-HCl mixtures.) Dotted lines correspond to a fit to eq 2 and 3, which gives $\Delta H = 19 \pm 7$ kJ/mol, $\Delta E = 67 \pm 16$ kJ/mol, $A \approx 1.9$ ns/(mPa s), $B \approx 8.3 \times 10^{-18}$ s.

internal viscosity but as a time scale for solvent-independent dynamics. Experimental estimates for σ may vary inconsistently from one protein to another (see above), but when analyzed in terms of a limiting time scale τ_{int} (rather than an internal viscosity σ), none of these results rule out nonzero values of τ_{int} in the range of nanoseconds to microseconds.

Because folding rates usually vary with temperature, we may expect τ_s in eq 2 to have a free energy of activation ΔG_s. This will cause the slope of $k_f^{-1}(\eta_s)$ vs η_s to decline as *T* increases. Figure 3 confirms that this slope does decrease slightly as the temperature rises from 17 to 30 °C. Remarkably, however, the figure also shows that the intercept k_f^{-1} ($\eta_s \rightarrow 0$) = τ_{int} falls roughly 3-fold over this temperature range, indicating that the internally controlled dynamics respond to another, relatively large energy scale. In fact, changes in τ_{int}, the intercept of $k_f^{-1}(\eta_s)$, appear to account for most of the temperature dependence of the folding rate at aqueous solvent viscosities (near 1 mPa s).

We can more quantitatively analyze this behavior by fitting the data of Figure 3 to eq 2 and assuming an explicitly Arrhenius *T* dependence for τ_s and τ_{int}:

$$\tau_s(T, \eta_s) = A\eta_s \exp(\Delta H/k_B T) \qquad (3a)$$

$$\tau_{int}(T) = B \exp(\Delta E/k_B T) \qquad (3b)$$

The dotted lines in the figure show the results of this four-parameter fit, which gives $\Delta H = 19 \pm 7$ kJ/mol and $\Delta E = 67 \pm 16$ kJ/mol, with $A \approx 1.88$ ns/(mPa s) and $B \approx 8.31 \times 10^{-18}$ s. Thus, even in water at 20 °C, $\tau_{int} \approx 6.2$ μs already exceeds $\tau_s \approx 5$ μs, and the $\sim$3−4-fold larger size of ΔE relative to ΔH confirms that τ_{int} has a far greater temperature sensitivity than does τ_s. The solvent insensitive dynamics essentially control both the time scale for folding in water

and its temperature dependence. The intrachain interactions responsible for internal friction involve a large energy scale in the compact, near-folded configurations. In fully unfolded cytochrome *c*, by contrast, the diffusional motions of the polypeptide scale directly with solvent viscosity and show little evidence that intrachain interaction energies affect the dynamics (*35*).

It is quite interesting to note that recent theoretical work actually anticipates a strong role for internal friction in proteins whose folding rate is insensitive to denaturant. The rate of a typical two-state folding process accelerates as the denaturant concentration decreases; however, Figure 1C shows that the rate of the late folding step studied here is insensitive to the denaturant concentration for [Gdn-HCl] < 2.5 M. Chan and co-workers (*23*, *41*) have proposed that flattening or rollover in plots of k_f vs denaturant may sometimes arise from kinetic trapping—a form of internal friction—within the polypeptide chain as the native state becomes extremely stable at low denaturant. That is, a rollover of the Chevron plot for a fast folding reaction may indicate the beginning of glassy dynamics, with accompanying strong internal friction effects. (A rollover in the rate-limiting folding step can usually be attributed to accumulation of transient intermediates.)

This suggests that we may consider the observed M → N folding time scale as the time required for a conformational search on the free energy landscape of the protein (*42*, *43*). This search time varies inversely with the effective diffusion constant D^*. In a rough landscape model, D^* depends in a non-Arrhenius fashion on the energy scale ϵ of the roughness, $D^* = D \exp[-(\epsilon / k_B T)^2]$ (*44*). If D^* controls the reorganization and folding times, τ_{int} and $k_f^{-1}(0)$, we can refit the data of Figure 3 using a non-Arrhenius temperature dependence for τ_{int}

$$\tau_{int}(T) = C \exp[(\epsilon/k_B T)^2] \qquad (4)$$

to obtain the "roughness" ϵ. This produces a virtually indistinguishable fit to the data, with $\epsilon = 9.1 \pm 1.1$ kJ/mol and $C \approx 6.2$ ps.

CONCLUSIONS

The rate of diffusional motion of an unfolded polypeptide chain through its solvent places one physical limit on the speed of protein folding. Reducing the solvent viscosity should therefore accelerate the process of folding but only until other phenomena—less strongly coupled to the solvent—begin to limit the folding rate. We have shown that in the limit of low solvent viscosities, the folding of a compact, late-stage folding intermediate of a 104 residue protein deviates from a simple Kramers-like dependence on solvent viscosity. The folding rate instead tends toward a solvent-viscosity-independent, although strongly temperature-dependent, limit of about 10^5 s^{-1}. Thus, while slower folding steps often exhibit a straightforward dependence on solvent friction, implying they are controlled directly by bulk diffusion in the solvent, the fastest folding dynamics in a compact system appear to decouple from the solvent at low viscosities. The observed reorganization rate, and its strong temperature dependence, provide a window into fundamental time and energy scales associated with diffusion of the polypeptide chain through the lower valleys of the free energy surface. Our data support the general view that upon the collapse of a polypeptide chain to a compact configuration, the energetics of intrachain interactions have a substantial slowing effect on the dynamics of reorganization into the folded configuration. They set the folding time scale at a few microseconds, a rate that is far slower than the simplest diffusional relaxations (~100 ns) of an ideal (noninteracting) unfolded polypeptide of similar length (*45*). Internal friction then sets an upper limit for folding speed that is quite different from the nanosecond diffusional speed limits associated with loop formation, hydrophobic collapse, and similar large-scale solvent-controlled motions of the chain (*45−52*). For proteins that fold at sufficiently high rates, internal friction appears capable of influencing folding rates at ordinary aqueous solvent viscosities, as suggested in some theoretical studies (*23*).

The fast time scale of these dynamics appears to explain why previous studies of protein folding at millisecond time scales failed to detect clear evidence for viscosity-independent, or internal friction-controlled, dynamics. Because most bulk diffusional motions, including contact formation and chain collapse, occur on time scales of at least tens or hundreds of microseconds, the present data suggest that internal friction effects will limit only the fastest protein folding rates. Shorter peptides appear to encounter little internal friction in forming elemental structures (*12*, *15*), but simulations (*23*) suggest that longer chains may exhibit internal frictional effects in their dynamics. For rapidly folding proteins, refolding in solvents of varying viscosity could cause a shift in the relative importance of different folding pathways, if some pathways couple more strongly to the solvent than do others. Strong internal friction effects in compact configurations also imply that internal friction could affect the dynamics of unfolded proteins artificially confined to sufficiently small volumes, such as by solvent crowding (*16*) or within molecular chaperones.

REFERENCES

1. Chrunyk, B. A., and Matthews, C. R. (1990) Role of diffusion in the folding of the α-subunit of tryptophan synthase from *Escherichia coli*, *Biochemistry 29*, 2149−2154.
2. Bhattacharyya, R. P., and Sosnick, T. R. (1999) Viscosity dependence of the folding kinetics of a dimeric and monomeric coiled coil, *Biochemistry 38*, 2601−2609.
3. Plaxco, K. W., and Baker, D. (1998) Limited internal friction in the rate-limiting step of a two-state protein folding reaction, *Proc. Natl. Acad. Sci. U.S.A. 95*, 13591−13596.
4. Jacob, M., Schindler, T., Balbach, J., and Schmid, F. X. (1997) Diffusion control in an elementary protein folding reaction, *Proc. Natl. Acad. Sci. U.S.A. 94*, 5622−5627.
5. Jacob, M., and Schmid, F. X. (1999) Protein folding as a diffusional process, *Biochemistry 38*, 13773−13779.
6. Jacob, M., Geeves, M., Holtermann, G., and Schmid, F. X. (1999) Diffusional barrier crossing in a two-state protein folding reaction, *Nat. Struct. Biol. 6*, 923−926.
7. Bilsel, O., and Matthews, C. R. (2000) Barriers in protein folding reactions, *Adv. Protein Chem. 53*, 153−207.
8. Kramers, H. A. (1940) Brownian motion in a field of force and the diffusion model of chemical reactions, *Physica 7*, 284−304.
9. Hanggi, P., Talkner, P., and Borkovec, M. (1990) Reaction-rate theory—50 years after Kramers, *Rev. Mod. Phys. 62*, 251−341.
10. Klimov, D. K., and Thirumalai, D. (1997) Viscosity dependence of the folding rates of proteins, *Phys. Rev. Lett. 79*, 317−320.
11. Portman, J. J., Takada, S., and Wolynes, P. G. (2001) Microscopic theory of protein folding rates. II. Local reaction coordinates and chain dynamics, *J. Chem. Phys. 114*, 5082−5096.

12. Zagrovic, B., and Pande, V. (2003) Solvent viscosity dependence of the folding rate of a small protein: Distributed computing study, *J. Comput. Chem. 24*, 1432−1436.

13. Tsong, T. Y., and Baldwin, R. L. (1978) Effects of solvent viscosity and different guanidine salts on kinetics of ribonuclease A chain folding, *Biopolymers 17*, 1669−1678.

14. Ladurner, A. G., and Fersht, A. R. (1999) Upper limit of the time scale for diffusion and chain collapse in chymotrypsin inhibitor 2, *Nat. Struct. Biol. 6*, 28−31.

15. Jas, G. S., Eaton, W. A., and Hofrichter, J. (2001) Effect of viscosity on the kinetics of alpha-helix and beta- hairpin formation, *J. Phys. Chem. B 105*, 261−272.

16. Silow, M., and Oliveberg, M. (2003) High concentrations of viscogens decrease the protein folding rate constant by prematurely collapsing the coil, *J. Mol. Biol. 326*, 263−271.

17. Yedgar, S., Tetreau, C., Gavish, B., and Lavalette, D. (1995) Viscosity dependence of O-2 escape from respiratory proteins as a function of cosolvent molecular-weight, *Biophys. J. 68*, 665−670.

18. Lavalette, D., Tetreau, C., Tourbez, M., and Blouquit, Y. (1999) Microscopic viscosity and rotational diffusion of proteins in a macromolecular environment, *Biophys. J. 76*, 2744−2751.

19. Ansari, A., Jones, C. M., Henry, E. R., Hofrichter, J., and Eaton, W. A. (1992) The role of solvent viscosity in the dynamics of protein conformational changes, *Science 256*, 1796−1798.

20. de Gennes, P. G. (1979) *Scaling Concepts in Polymer Physics*, Cornell University Press, Ithaca, NY.

21. Manke, C. W., and Williams, M. C. (1985) Internal viscosity of polymers and the role of solvent resistance, *Macromolecules 18*, 2045−2051.

22. Ansari, A. (1999) Langevin modes analysis of myoglobin, *J. Chem. Phys. 110*, 1774−1780.

23. Kaya, H., and Chan, H. S. (2002) Towards a consistent modeling of protein thermodynamic and kinetic cooperativity: How applicable is the transition state picture to folding and unfolding?, *J. Mol. Biol. 315*, 899−909.

24. Grote, R. F., and Hynes, J. T. (1980) The stable states picture of chemical reactions. 2. Rate constants for condensed and gas-phase reaction models, *J. Chem. Phys. 73*, 2715−2732.

25. Qiu, L. L., and Hagen, S. J. (2004) A limiting speed for protein folding at low solvent viscosity, *J. Am. Chem. Soc. 126*, 3398−3399.

26. Neidigh, J. W., Fesinmeyer, R. M., and Andersen, N. H. (2002) Designing a 20-residue protein, *Nat. Struct. Biol. 9*, 425−430.

27. Qiu, L. L., Pabit, S. A., Roitberg, A. E., and Hagen, S. J. (2002) Smaller and faster: The 20-residue Trp-cage protein folds in 4 μs, *J. Am. Chem. Soc. 124*, 12952−12953.

28. Latypov, R. F., Maki, K., Cheng, H., Luck, S. D., and Roder, H. (2003) Folding mechanism of reduced cytochrome *c*: Equilibrium properties in the presence and absence of carbon monoxide, *J. Mol. Biol.*, to be submitted.

29. Jones, C. M., Henry, E. R., Hu, Y., Chan, C. K., Luck, S. D., Bhuyan, A., Roder, H., Hofrichter, J., and Eaton, W. A. (1993) Fast events in protein-folding initiated by nanosecond laser photolysis, *Proc. Natl. Acad. Sci. U.S.A. 90*, 11860−11864.

30. Bhuyan, A. K., and Kumar, R. (2002) Kinetic barriers to the folding of horse cytochrome *c* in the reduced states, *Biochemistry 41*, 12821−12834.

31. George, P., and Schejter, A. (1964) Reactivity of ferrocytochrome C with iron-binding ligands, *J. Biol. Chem. 239*, 1504.

32. Pascher, T., Chesick, J. P., Winkler, J. R., and Gray, H. B. (1996) Protein folding triggered by electron transfer, *Science 271*, 1558−1560.

33. Sato, S., Sayid, C. J., and Raleigh, D. P. (2000) The failure of simple empirical relationships to predict the viscosity of mixed aqueous solutions of guanidine hydrochloride and glucose has

34. Englander, S. W., Calhoun, D. B., and Englander, J. J. (1987) Biochemistry without oxygen, *Anal. Biochem. 161*, 300−306.

35. Hagen, S. J., Carswell, C. W., and Sjolander, E. M. (2001) Rate of intrachain contact formation in an unfolded protein: Temperature and denaturant effects, *J. Mol. Biol. 305*, 1161−1171.

36. Hagen, S. J., Latypov, R. F., Dolgikh, D. A., and Roder, H. (2002) Rapid intrachain binding of Histidine-26 and Histidine-33 to heme in unfolded ferrocytochrome *c*, *Biochemistry 41*, 1372−1380.

37. Hagen, S. J., Hofrichter, J., and Eaton, W. A. (1997) Rate of intrachain diffusion of unfolded cytochrome *c*, *J. Phys. Chem. B 101*, 2352−2365.

38. Waldburger, C. D., Jonsson, T., and Sauer, R. T. (1996) Barriers to protein folding: Formation of buried polar interactions is a slow step in acquisition of structure, *Proc. Natl. Acad. Sci. U.S.A. 93*, 2629−2634.

39. Massa, D. J., Schrag, J. L., and Ferry, J. D. (1971) Dynamic viscoelastic properties of polystyrene in high-viscosity solvents−Extrapolation to infinite dilution and high-frequency behavior, *Macromolecules 4*, 210.

40. Osaki, K., and Schrag, J. L. (1971) Viscoelastic properties of polymer solutions in high-viscosity solvents and limiting high-frequency behavior. 1. Polystyrene and poly(alpha-methylstyrene), *Polym. J. 2*, 541.

41. Chan, H. S., Shimizu, S., and Kaya, H. (2004) Cooperativity principles in protein folding, *Methods Enzymol. 380*, 350−379.

42. Bryngelson, J. D., Onuchic, J. N., Socci, N. D., and Wolynes, P. G. (1995) Funnels, pathways, and the energy landscape of protein-folding−A synthesis, *Proteins: Struct., Funct., Genet. 21*, 167−195.

43. Socci, N. D., Onuchic, J. N., and Wolynes, P. G. (1996) Diffusive dynamics of the reaction coordinate for protein folding funnels, *J. Chem. Phys. 104*, 5860−5868.

44. Zwanzig, R. (1988) Diffusion in A Rough Potential, *Proc. Natl. Acad. Sci. U.S.A. 85*, 2029−2030.

45. Qiu, L. L., Zachariah, C., and Hagen, S. J. (2003) Fast chain contraction during protein folding: "Foldability" and collapse dynamics, *Phys. Rev. Lett. 90*, art 168103.

46. Hagen, S. J., Hofrichter, J., Szabo, A., and Eaton, W. A. (1996) Diffusion-limited contact formation in unfolded cytochrome *c*: Estimating the maximum rate of protein folding, *Proc. Natl. Acad. Sci. U.S.A. 93*, 11615−11617.

47. Bieri, O., Wirz, J., Hellrung, B., Schutkowski, M., Drewello, M., and Kiefhaber, T. (1999) The speed limit for protein folding measured by triplet−triplet energy transfer, *Proc. Natl. Acad. Sci. U.S.A. 96*, 9597−9601.

48. Lapidus, L. J., Eaton, W. A., and Hofrichter, J. (2000) Measuring the rate of intramolecular contact formation in polypeptides, *Proc. Natl. Acad. Sci. U.S.A. 97*, 7220−7225.

49. Chang, I. J., Lee, J. C., Winkler, J. R., and Gray, H. B. (2003) The protein-folding speed limit: Intrachain diffusion times set by electron-transfer rates in denatured Ru(NH3)(5)(His-33)-Zn-cytochrome *c*, *Proc. Natl. Acad. Sci. U.S.A. 100*, 3838−3840.

50. Yang, W. Y., and Gruebele, M. (2003) Folding at the speed limit, *Nature 423*, 193−197.

51. Zhu, Y., Alonso, D. O. V., Maki, K., Huang, C. Y., Lahr, S. J., Daggett, V., Roder, H., DeGrado, W. F., and Gai, F. (2003) Ultrafast folding of alpha(3): A de novo designed three-helix bundle protein, *Proc. Natl. Acad. Sci. U.S.A. 100*, 15486−15491.

52. Mayor, U., Guydosh, N. R., Johnson, C. M., Grossmann, J. G., Sato, S., Jas, G. S., Freund, S. M. V., Alonso, D. O. V., Daggett, V., and Fersht, A. R. (2003) The complete folding pathway of a protein from nanoseconds to microseconds, *Nature 421*, 863−867.

important implications for the study of protein folding, *Protein Sci. 9*, 1601−1603.